On the Practical Implementation of Propagation Delay and Clock Skew Compensated High-Precision Time Synchronization Schemes with Resource-Constrained Sensor Nodes in Multi-Hop Wireless Sensor Networks

Xintao Huan[a], Kyeong Soo Kim[a,*]

[a]*Department of Electrical and Electronic Engineering, Xi'an Jiaotong-Liverpool University, Suzhou 215123, Jiangsu Province, P. R. China*

Abstract

In wireless sensor networks (WSNs), implementing an energy-efficient, high-precision time synchronization scheme on resource-constrained sensor nodes is challenging but essential to long-running applications for accurate environment monitoring and detection of important events, often covering a large area in the field. Our investigation of the practical implementation on a real testbed of the state-of-the-art WSN time synchronization scheme based on the asynchronous source clock frequency recovery and the reverse two-way message exchange, which can compensate for both propagation delay and clock skew for higher precision and energy efficiency, reveals that its performance on battery-powered, low-complexity sensor nodes is not up to that predicted from simulation experiments due to the limited precision floating-point arithmetic of sensor nodes. Noting the lower computational capability of typical sensor nodes and its impact on time synchronization, we propose an asymmetric high-precision time synchronization scheme that can provide high-precision time synchronization even with resource-constrained sensor nodes in multi-hop WSNs. In the proposed scheme, all synchronization-related computations are done at the head node equipped with abundant computing and power resources, while the sensor nodes are responsible for timestamping only to further release their computational burdens. Experimental results with a testbed based on TelosB motes running TinyOS demon-

---

[*]Corresponding author
  Email address: Kyeongsoo.Kim@xjtlu.edu.cn (Kyeong Soo Kim)

strate that the proposed time synchronization scheme can avoid time synchronization errors resulting from the single-precision floating-point arithmetic of the resource-constrained sensor nodes and achieve microsecond-level time synchronization accuracy in multi-hop WSNs.

Keywords: Asymmetric time synchronization, reverse two-way message exchange, multi-hop wireless sensor networks

1. Introduction

High-precision time synchronization is essential to the runtime collaborative applications for wireless sensor networks (WSNs), including time-based channel sharing and media access control (MAC) protocols [1], coordinated duty cycling mechanisms [2], and device-free wireless sensing for human activity and gesture recognition [3, 4]. Considering the increasing number of WSN deployments for a variety of applications, most of which are based on multi-hop topologies with resource-constrained sensor nodes, achieving high-precision time synchronization in multi-hop networks while lowering the computational requirements and energy consumption at sensor nodes is crucial in designing WSN time synchronization schemes.

In [5], we have proposed a novel energy-efficient time synchronization scheme based on the asynchronous source clock frequency recovery (SCFR) [6] and the reverse two-way message exchange as illustrated in Fig. 1, which we call *EE-ASCFR* in short from now on. Unlike the conventional WSN time synchronization schemes where sensor nodes are responsible for most of the clock estimation procedures (e.g., [7, 8, 9, 10, 11, 12, 13, 14]), EE-ASCFR suits the resource-constrained sensor nodes, because sensor nodes are relieved from the task of clock offset estimation that is moved to and done in a centralized manner at the head node[1]; in EE-ASCFR, the logical clocks of sensor nodes are synchronized to the reference clock of the head node in frequency through the asynchronous SCFR, but they could run possibly with different and independent offsets. Such redistribution of the synchronization tasks reduces not only the energy consumption through the reduced number of message transmissions in the two-way message exchange but also the computational complexity of sensor nodes. Extensive simulation experiments demonstrate that EE-ASCFR can provide sub-microsecond-level accuracy

---

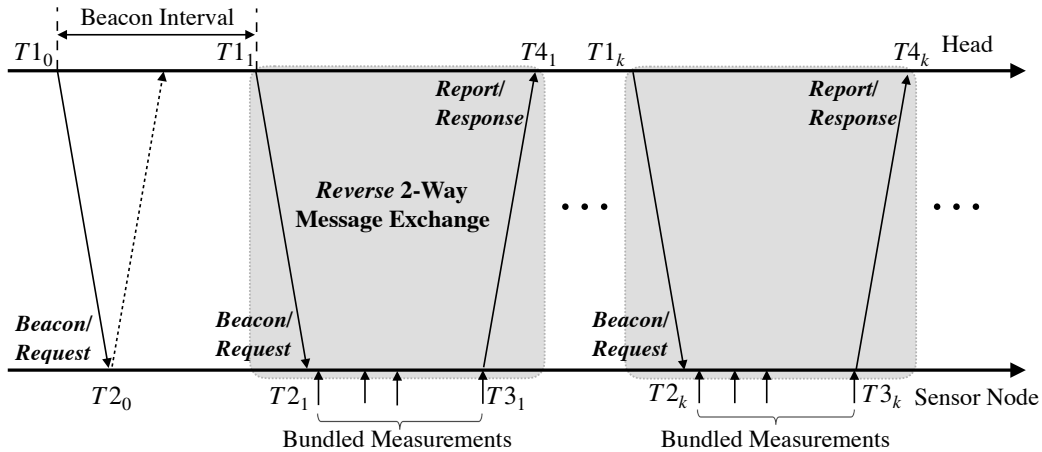[1]A head node is also called a sink node in the literature.

Figure 1: Reverse two-way message exchange with optional bundling of measurements introduced in [5].

while significantly reducing the number of message exchanges required for time synchronization. Note that the actual performance of EE-ASCFR on a real testbed was not evaluated at all in [5], which is the starting point of our investigation reported in this paper.

To evaluate the actual performance of the high-precision time synchronization schemes, we implemented EE-ASCFR on TelosB [15] motes running TinyOS [16] and investigated its time synchronization performance on a real testbed. During the investigation, we found that the limited computing capability of the sensor nodes could result in cumulative synchronization errors in EE-ASCFR. This is because the estimation of the frequency ratio and the maintenance of the logical clock require floating-point divisions and the limited floating-point precision of the resource-constrained sensor nodes—i.e., 32-bit single-precision on TinyOS—could result in cumulative synchronization errors.

Note that, the 32-bit single-precision floating-point representation is the floating-point standard not only of most resource-constrained WSN platforms such as MicaZ [17], Iris [18] and TelosB [15] but also of most Arduino platforms [19]. The latter platforms are extremely prevalent in Internet of things (IoT) prototyping, and their computing and power resources are also quite limited. Moreover, the high-precision time synchronization is also critical to collaborative IoT applications. Consequently, minimizing the computing requirements of high-precision time synchronization schemes for the resource-

3

constrained platforms is a timely and critical research topic for the success of WSNs and IoT in the future.

Based on the results of the investigation of EE-ASCFR time synchronization performance on a real WSN testbed, in this paper we study the practical implementation of proposed delay and clock skew compensated high-precision time synchronization schemes with resource-constrained WSN sensor nodes. The major contributions of our work in this paper can be summarized as follows:

- First, we systematically investigate and analyze the impact of the precision loss resulting from the use of single-precision floating-point format at resource-constrained sensor nodes on the time synchronization performance of EE-ASCFR and show the correlation between the computational error in time synchronization and the aforementioned precision loss.

- Second, based on our investigation and analysis of the impact of the precision loss on time synchronization, we propose an improved WSN time synchronization scheme called *asymmetric high-precision time synchronization (AHTS)*, which can provide microsecond-level accuracy even with resource-constrained sensor nodes by relieving them of all time synchronization tasks but timestamping. We also present its multi-hop extension to make it scalable in actual deployments.

- Finally, we present the results of experiments on a real WSN testbed based on TelosB motes—one of the representative WSN platforms— running TinyOS to demonstrate the effectiveness of the proposed scheme in both single-hop and multi-hop scenarios.

The rest of this paper is organized as follows: The impact of the limited precision floating-point arithmetic on time synchronization at resource-constrained sensor nodes is investigated in detail in Section 2. The proposed AHTS and its extension to multi-hop topologies are described in Section 3. The results of experiments with a real testbed for a comparative analysis of the performance of the proposed AHTS and EE-ASCFR in both single-hop and multi-hop topologies are presented in Section 4. Section 5 concludes our work with directions for future work.

2. Impact of Limited Precision Floating-Point Arithmetic on Time Synchronization

We begin our investigation of the impact of limited precision floating-point arithmetic on time synchronization at resource-constrained sensor nodes with EE-ASCFR, the state-of-the-art time synchronization scheme proposed in [5], which compensates for both propagation delay and clock skew to provide sub-microsecond-level synchronization accuracy. In [5], the performance of EE-ASCFR is evaluated based on mathematical analyses and simulation experiments but not with a real testbed. To evaluate its actual performance on the resource-constrained sensor nodes, therefore, we implemented and evaluated it on a WSN testbed based on TelosB motes running TinyOS.

As discussed in Section 1, EE-ASCFR focuses on an asymmetric WSN with a head node with higher computing and power resources and multiple battery-powered, low-complexity sensor nodes. The asymmetric scenario of EE-ASCFR represents the most common WSN applications such as environment monitoring. As the hardware clocks of the sensor nodes are not ideal, they can possibly have different clock frequencies and offsets with respect to the reference clock.

In EE-ASCFR, the first-order affine clock model is used to model the hardware clock T_i of a sensor node i with respect to the reference clock t of the head node [5]: For $i \in [0, 1, \ldots, N-1]$,

$$T_i(t) = (1 + \epsilon_i)\, t + \theta_i, \tag{1}$$

where N is the number of sensor nodes and $\epsilon_i \in \mathbb{R}$ and $\theta_i \in \mathbb{R}$ denote the clock skew[2] and the clock offset between the reference clock and the hardware clock of a sensor node i, respectively. Based on the hardware clock T_i, the logical clock $\mathscr{T}_i$ used for timestamping at the sensor node can be described as follows: For $t_k < t \leq t_{k+1}$ ($k = 0, 1, \ldots$),

$$\mathscr{T}_i\Big(T_i(t)\Big) = \mathscr{T}_i\Big(T_i(t_k)\Big) + \frac{T_i(t) - T_i(t_k)}{1 + \hat{\epsilon}_{i,k}} - \hat{\theta}_{i,k}, \tag{2}$$

---

[2]A clock skew is defined as a normalized clock frequency difference between two clocks, and its typical value for clocks based on quartz crystal oscillators is of the order of tens of ppm (i.e., $\epsilon_i \ll 1$) [5]. Note that $(1 + \epsilon_i) \in \mathbb{R}_+$ in (1) is a clock frequency ratio.
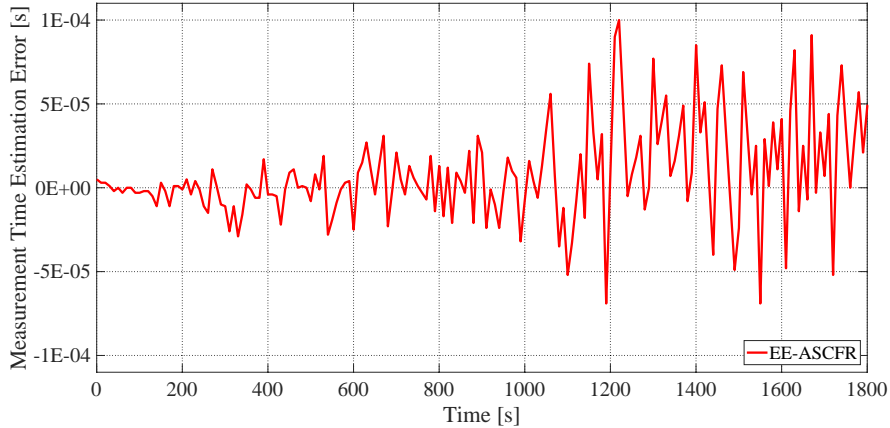
Figure 2: Measurement time estimation errors of EE-ASCFR with SI of 1 s.

where t_k is the reference time for the kth synchronization, $\hat{\epsilon}_{i,k}$ and $\hat{\theta}_{i,k}$ are the estimated clock skew and offset from the kth synchronization. Note that $\hat{\theta}_{i,k}$ is set to 0 in (2), which is compensated at the head node as described in [5]; the sensor node only synchronizes the frequency of the logical clock to that of the reference clock using asynchronous SCFR scheme. According to the reverse two-way message exchange shown in Fig. 1, the clock frequency ratio—i.e., $1+\epsilon_k$ in (1)—is estimated as $(T2_k-T2_0)/(T1_k-T1_0)$, where the timestamps of Ti_j ($i{=}1,2$ and $j{\geq}0$) are recorded during the jth synchronization.

Fig. 2 shows the measurement time estimation errors from the experiment with the testbed for a period of 1800 s, where the synchronization interval (SI) is set to 1 s and 5 measurements are generated and bundled together in a "Report/Response" message to the head node in each SI. As shown in Fig. 2, the absolute value of measurement time estimation error of EE-ASCFR gradually increases from around 2 μs to 100 μs over the period of 1200 s, which indicates that, as will be discussed shortly, the limited precision in floating-point arithmetic of the resource-constrained sensor nodes (i.e., 32-bit single-precision in this case) has negative impacts on the time synchronization performance.

Note that, when proposing the ratio-based time synchronization protocol (RSP) [20], i.e., a variation of flooding time synchronization protocol (FTSP) [8] based on a simpler ratio-based clock estimation method, the au-

6

thors discuss the impact of computational errors resulting from the limited precision floating-point arithmetic on time synchronization in a qualitative way. Specifically, they claim that a smaller synchronization time interval could lead to larger computational errors, while a larger synchronization time interval, too, may negatively affect time synchronization due to the clock drift over a long period. This means that we need to address the impact of the computational errors due to the limited-precision floating-point arithmetic in designing the high-precision time synchronization schemes for the resource-constrained sensor nodes.

To systematically investigate the cause of the increase of the measurement time estimation errors over time in EE-ASCFR, we revisit the arithmetic computations involved with the logical clock updates in (2) at the sensor node. During the simulation experiments reported in [5], the division of floating-point numbers (e.g., the division of $T_i(t) - T_i(t_k)$ by $1 + \hat{\epsilon}_{i,k}$ in (2)) does not incur much precision loss as the arithmetic precision supported by most personal computers (PCs) and workstations is high enough (i.e., 64-bit double-precision floating-point type). For typical WSN platforms based on a low-cost microcontroller unit (MCU) and limited memory space, however, floating-point type is generally limited to 32-bit single-precision, which may result in significant precision loss. As described in [21], implementing high-precision synchronization schemes requiring floating-point division in WSNs has to be discreet due to the hardware limitations of the underlying platforms. In case of EE-ASCFR, because the logical clock updates at sensor nodes in (2) requires accurate floating-point division and has a recursive nature, the impact of the computational errors on the logical clock is accumulated over time.

To avoid the recursive nature of (2) in EE-ASCFR and simplify the quantification of the impact of limited precision on time synchronization, we propose an improved logical clock update equation as follows:

$$\mathscr{T}_i\Big(T_i(t)\Big) = \mathscr{T}_i\Big(T_i(t_0)\Big) + \frac{T_i(t) - T_i(t_0)}{1 + \hat{\epsilon}_{i,k}}, \tag{3}$$

where the current logical clock is updated based on the value of the logical clock at the first time synchronization, instead of its value at the previous time synchronization (i.e., $\mathscr{T}_i(T_i(t_k))$), and the time duration since the first time synchronization divided by the estimated clock frequency ratio. Even though there is no recursive term in (3), however, the experiments with the real testbed show that this improved logical clock update equation still results

7

in cumulative errors caused by the precision loss involved with the division by $1 + \hat{\epsilon}_{i,k}$ (i.e., the second term in RHS of (3)).

The impact of the precision loss in EE-ASCFR can be analyzed as follows: Because $\hat{\epsilon}_{i,k} \ll 1$ in general, the second term in RHS of (3) can be approximated by its first-order Taylor polynomial, i.e.,

$$\frac{T_i(t) - T_i(t_0)}{1 + \hat{\epsilon}_{i,k}} \approx \Big(T_i(t) - T_i(t_0)\Big) \times (1 - \hat{\epsilon}_{i,k}). \tag{4}$$

Let ϵ be the precision loss for the clock skew $\hat{\epsilon}_{i,k}$, i.e.,

$$\epsilon \triangleq \hat{\epsilon}_{i,k} - \hat{\epsilon}_{i,k}^{LP}, \tag{5}$$

where $\hat{\epsilon}_{i,k}^{LP}$ denotes the actual, imprecise value of the clock skew in implementation due to the limited precision. Then, the computational error Ψ due to the precision loss can be described as follows:

$$\begin{aligned} \Psi &\triangleq \Big(T_i(t) - T_i(t_0)\Big) \times (1 - \hat{\epsilon}_{i,k}) - \Big(T_i(t) - T_i(t_0)\Big) \times (1 - \hat{\epsilon}_{i,k}^{LP}) \\ &= \Big(T_i(t) - T_i(t_0)\Big) \times (\hat{\epsilon}_{i,k}^{LP} - \hat{\epsilon}_{i,k}) \\ &= -\Big(T_i(t) - T_i(t_0)\Big)\epsilon. \end{aligned} \tag{6}$$

(6) shows that, given the precision loss ϵ, the computational error Ψ is proportional to the time duration since the first time synchronization. This means that the computational error becomes larger as the logical clock is continuously updated, because the time duration since the first time synchronization—i.e., $T_i(t) - T_i(t_0)$—increases. Note that the computational error Ψ in (6) is independent of SI (i.e., $T_i(t_i) - T_i(t_{i-1})$), which means that reducing SI does not mitigate the impact of limited precision floating-point arithmetic on time synchronization.

To quantify the impact of the precision loss, we turn back to the definition of the floating-point formats in IEEE standard 754 [22]. According to the definitions of the 32-bit floating-point and decimal interchange format parameters in this standard, 7-digit precision is provided for decimal numbers. As nesC language [23], which is used to build applications on the TinyOS platform, is basically the extension of the standard C language and follows the IEEE standard 754 as described in [24], the decimal numbers represented by nesC 32-bit floating-point type provide the limited precision of 7 digits.

Note that the highest clock resolution provided by TinyOS is $1\,\mu s$, which limits the precision of all time synchronization schemes implemented on the TinyOS platform, including EE-ASCFR. Considering the microsecond-level synchronization limit of the TinyOS and the SI of $10\,s$ as an example, $10^7\,\mu s$ is the actual value involved in the computation of logical clock in (2) (i.e., the difference between the two timestamps). In the worst case, the loss of the precision in the estimated frequency ratio, whose true value is very close to one, would be 10^{-7} (i.e., ϵ).

3. Asymmetric High-Precision Time Synchronization (AHTS)

Based on the results of the investigation of the impact of limited precision floating-point arithmetic on time synchronization at resource-constrained sensor nodes with EE-ASCFR in Section 2, here we propose AHTS that can achieve microsecond-level time synchronization accuracy even with resource-constrained sensor nodes in multi-hop WSNs. We first describe its system architecture and basic operations and then discuss its extension to multi-hop topologies.

3.1. System Architecture and Basic Operations

To address the issues resulting from the limited precision floating-point arithmetic at resource-constrained sensor nodes, we move all the time synchronization tasks of sensor nodes except timestamping to the head[3] in AHTS: Specifically, as shown in Fig. 3, the logical clock translator described in (3) and the frequency ratio estimator (i.e., the cumulative ratio (CR) estimator in [6])—which run at sensor nodes in EE-ASCFR—are now part of the time synchronization tasks of the head.

This redistribution of time synchronization tasks between the head and sensor nodes leaves just timestamping (i.e., the "MAC-layer Time Recorder" in Fig. 3) to sensor nodes. As a result, all floating-point arithmetic operations required by the clock estimation procedures are done at the head with abundant computing and power resources (including 64-bit double-precision floating-point arithmetic). Based on this revised system architecture, AHTS operates as follows:

---

[3]From now on, we collectively call the head node and the monitoring center (i.e., a workstation or a server) connected to it as the head.
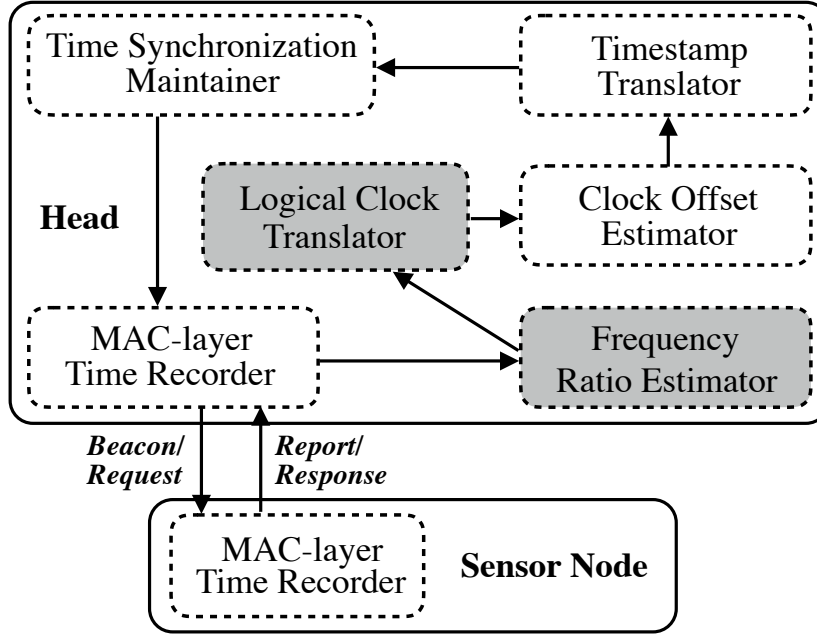
Figure 3: System architecture of AHTS for resource-constrained wireless sensor networks.

In the beginning of AHTS operation, the time synchronization maintainer at the head triggers the time synchronization process, and a hardware clock timestamp $T1$ is recorded by the MAC-layer time recorder and sent to sensor nodes via a *Beacon/Request* message. When a sensor node receives the *Beacon/Request* message, it records the value of its own hardware clock $T2$. Note that, in the reverse two-way message exchange as implemented in EE-ASCFR, $T2_0$ shown in Fig. 1 is not required by the head as the estimation of the clock frequency ratio is done at the sensor node. In AHTS, however, $T2_0$ is essential for the head to estimate the clock frequency ratio. Consequently, $T2_0$ has to be delivered from the sensor node to the head either through one additional message after the initial *Beacon/Request* message (i.e., the dotted line in Fig. 1) or embedded in the first *Report/Response* message later.

When a measurement event occurs, the sensor node records a timestamp T_m with respect to its own hardware clock. A *Response/Report* message is transmitted to the head, carrying the measurement timestamp T_m and the most recently generated $T2$ together with the hardware clock timestamp $T3$ of its own transmission time. When receiving the *Response/Report* message from a sensor node, the head records a timestamp $T4$ using its MAC-layer

10

time recorder. The frequency ratio estimator calculates the clock frequency ratio based on the differences of current $T2$ and $T1$ to the initial ones (i.e., $T2_0$ and $T1_0$) by employing 64-bit double-precision floating-point type[4], which has the precision of 16 digits [22].

Afterwards, the clock offset estimator estimates the clock offset based on the reverse two-way message exchange as in EE-ASCFR. With the estimated clock frequency ratio and clock offset, the timestamp translator finally converts the value of the measurement timestamp T_m, which is based on the hardware clock of the sensor node, into that based on the reference clock at the head.

Note that, because AHTS is based on the same reverse two-way message exchange as EE-ASCFR, it can properly compensate for propagation delay that is ignored in the time synchronization schemes based on the one-way message dissemination (e.g., FTSP and RSP). In addition to the propagation delay, the interrupt delay—i.e., the delay between the transmission and reception interrupts of a message at a sender and a receiver—is also compensated as part of the two-way message exchange.

3.2. Multi-Hop Time Synchronization

In [5], the extension of EE-ASCFR to a hierarchical structure for network-wide, multi-hop time synchronization is sketched based on packet-relaying and time-translating gateways, but no implementation details are provided. Here we discuss the multi-hop extension of AHTS and the details of its implementation.

The conventional multi-hop one-way and two-way time synchronization schemes are shown in Fig. 4 (a) and (b), respectively. As shown in the figure, compared to the time synchronization schemes based on the one-way message dissemination, those based on the two-way message exchange (e.g., timing-sync protocol for sensor networks (TPSN) [7]) require one additional message at each hop to acquire four timestamps: For a flat n-hop network, for instance, we need n synchronization messages and $2n$ timestamps for the one-way scheme but $2n$ synchronization messages and $4n$ timestamps for the two-way scheme.

In terms of the number of message transmissions, the conventional multi-hop one-way scheme is more efficient but at the expense of relatively lower

---

[4]The 64-bit double-precision floating-point type is also named as *double* type in common programming languages.
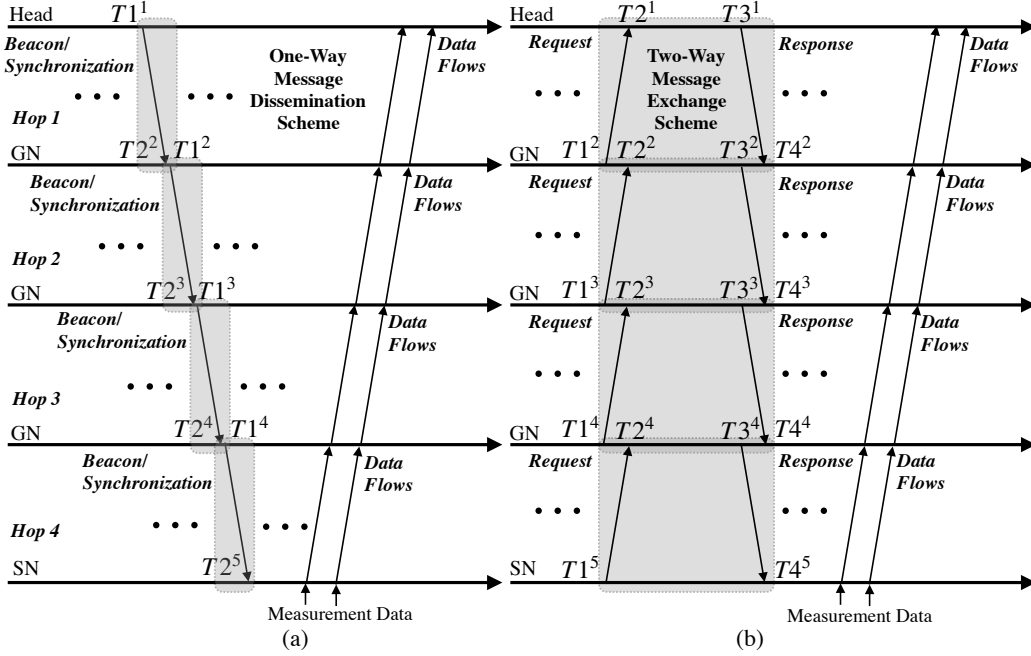
Figure 4: Conventional multi-hop time synchronization schemes based on (a) the one-way message dissemination and (b) the two-way message exchange.

time synchronization accuracy resulting from the lack of propagation delay compensation. For high-precision time synchronization (e.g., microsecond-level), by the way, the impact of propagation delay, which is negligible in a single-hop network, could be accumulated through per-hop forwarding and no longer negligible in a multi-hop network. Therefore, the propagation delay should be properly compensated for in the high-precision multi-hop time synchronization schemes.

Note that both EE-ASCFR and AHTS, i.e., the improved version of EE-ASCFR, address the issue of the increased number of message transmissions through the reverse two-way message exchange and the embedment of measurement data in time synchronization messages, which could reduce the number of message transmissions to that of the conventional one-way schemes as shown in Fig. 5 while compensating for the propagation delay as in the conventional two-way schemes. In addition, both EE-ASCFR and AHTS could further reduce the number of message transmissions through measurement data bundling, which is also shown in Fig. 5.

As for the processing of the timestamps related with the reverse two-way
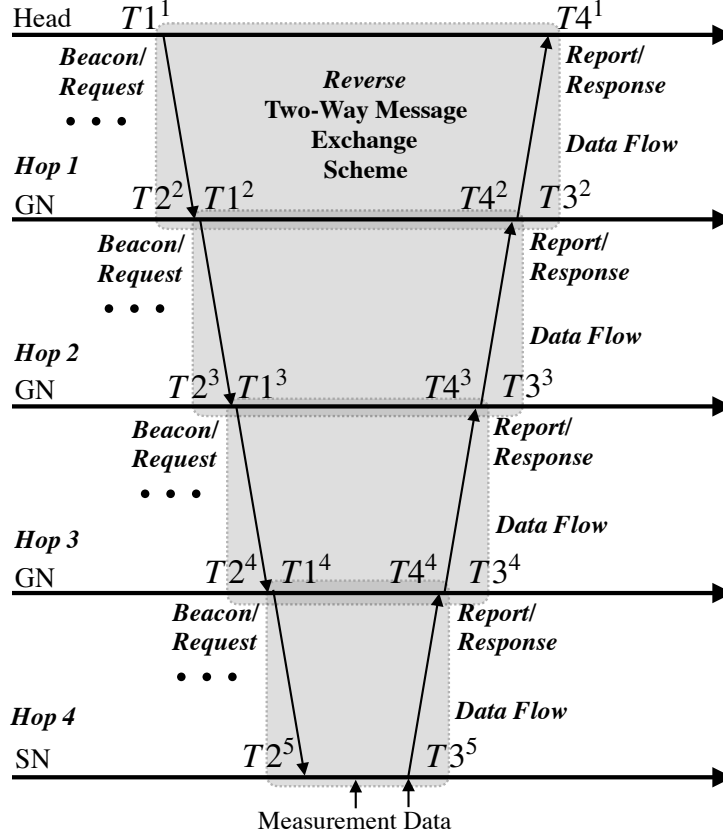
Figure 5: Multi-hop extension of time synchronization schemes based on the reverse two-way message exchange with optional bundling of measurement data.

message exchange over multiple hops, we adopt the time-translation approach described in [5] but again move its processing from the intermediate gateway nodes to the head in order to address the increased energy consumption and processing at the gateway nodes that are likely to be battery-powered like other sensor nodes. Specifically, each hop of the multi-hop network maintains the same timestamping procedure as in the single-hop network (e.g., $T1^3$, $T2^4$, $T3^4$, and $T4^3$ for Hop 3, and $T1^4$, $T2^5$, $T3^5$, and $T4^4$ for Hop 4 in Fig. 5). Then the upper node—i.e., the node working as a gateway for its lower nodes in the original time-translating gateway approach in EE-ASCFR—just transfers the set of the four collected timestamps to the head, which eventually handles the translation of the measurement times embedded in a packet with the timestamps based on the logical clocks and the offsets for the two nodes.

In this way, we eliminate the impact of any extra delays on time synchronization such as packet delays resulting from queueing and MAC operations, which are accumulated through per-hop forwarding in multi-hop networks and could severely affect the other approach based on packet relaying gateway nodes as discussed in [5].

4. Experimental Results

We carry out a comparative analysis of the time synchronization performance of EE-ASCFR and the proposed AHTS based on a series of experiments for both single-hop and multi-hop scenarios with a real WSN testbed consisting of TelosB motes running TinyOS.

As discussed in Section 2, the implementation of EE-ASCFR on a real WSN testbed reveals the significant impact of the limited precision floating-point arithmetic of resource-constrained sensor nodes on time synchronization performance. The focus of the experiments and their analyses, therefore, is put on how the proposed AHTS addresses the issue of the precision loss resulting from the use of single-precision floating-point format at resource-constrained sensor nodes in time synchronization.
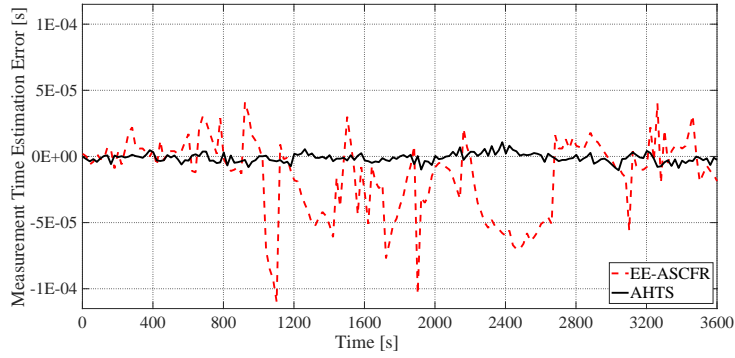
4.1. Single-Hop Scenario

First, we consider a single-hop WSN with one head and one sensor node. The experiments are run over a period of $3600\,\mathrm{s}$ with three different values of SI, i.e., $1\,\mathrm{s}$, $10\,\mathrm{s}$ and $100\,\mathrm{s}$. The number of bundled measurements is set to 5 for all the experiments. Fig. 6 shows the measurement time estimation errors of EE-ASCFR and AHTS, and Table 1 summarizes the mean absolute error (MAE) and the mean squared error (MSE) of their measurement time estimation.

The results of Fig. 6 and Table 1 show that the measurement time synchronization errors of AHTS are stable and much smaller than those of EE-ASCFR over the observation period for all three values of SI, which demonstrates that the proposed AHTS successfully addresses the issue of precision loss in the logical clock update discussed in Section 2.
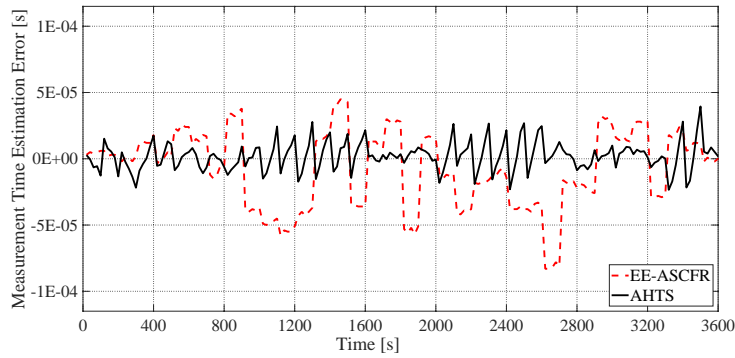
The effect of SI on time synchronization is more visible in AHTS than EE-ASCFR, especially for the SI of $100\,\mathrm{s}$, which may result from a larger range of clock drift over a longer period of time by the sensor node's hardware clock based on a cheap quartz crystal oscillator. In case of EE-ASCFR, the
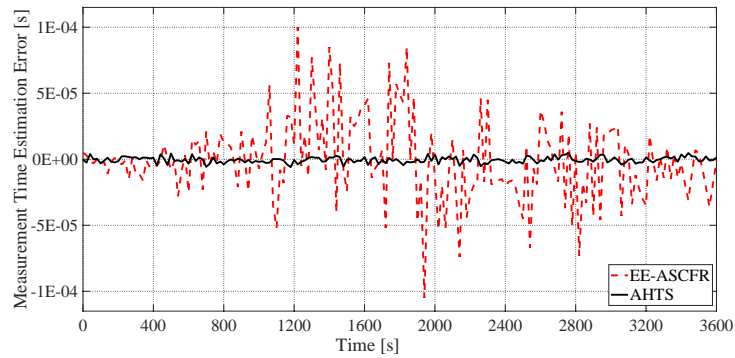
Figure 6: Measurement time estimation errors of EE-ASCFR and AHTS with SI of (a) 1 s, (b) 10 s and (c) 100 s for the single-hop scenario.

effect of SI becomes less visible as time goes on (i.e., over 800 s), because it

15

Table 1: MAE and MSE of Measurement Time Estimation of EE-ASCFR and AHTS for the Single-Hop Scenario

Synchronization Scheme		MAE [1]	MSE [1]
EE-ASCFR	SI = 100 s	2.7276E-05	1.0391E-09
	SI = 10 s	2.5182E-05	1.1559E-09
	SI = 1 s	2.4069E-05	1.0095E-09
AHTS	SI = 100 s	8.4225E-06	1.2524E-10
	SI = 10 s	2.3385E-06	9.1694E-12
	SI = 1 s	1.8166E-06	5.2094E-12

[1] The samples measured between 360 s (i.e., a tenth of the total observation period) and 3600 s are employed to avoid the effect of a transient period.

is overshadowed by that of the aforementioned precision loss.

Overall, the experimental results from the single-hop scenario show that the proposed AHTS successfully addresses the issue of the precision loss in time synchronization at resource-constrained sensor nodes and can deliver microsecond-level time synchronization accuracy.

4.2. Multi-Hop Scenario

To investigate the effect of the number of hops on time synchronization in multi-hop topologies, we also consider a multi-hop WSN with one head and three sensor nodes. The experiments are run over a period of 3600 s as in the single-hop scenario, but the SI value is fixed to 1 s. For a fair comparison of the time synchronization performance of sensor nodes in the multi-hop scenario, each sensor node bundles only its own measurement and synchronization data with the number of bundled measurements set to 5 as in the single-hop scenario. Fig. 7 shows the measurement time estimation errors of AHTS for different number of hops, and Table 2 summarizes the MAE and the MSE of the measurement time estimation.

From Table 2, we found that the MAE of measurement time estimation for Hop 1 is 2.1774 μs, which is close to that of the single-hop scenario (i.e., 1.8166 μs). We also found that, due to the layer-by-layer translation of the multi-hop extension, the MAE of measurement time estimation slightly increases as the hop count increases, which amounts to about 0.2 μs per hop. Likewise, the measurement time estimation errors in Fig. 7 show more fluctuations for Hop 2 and Hop 3 than Hop 1.
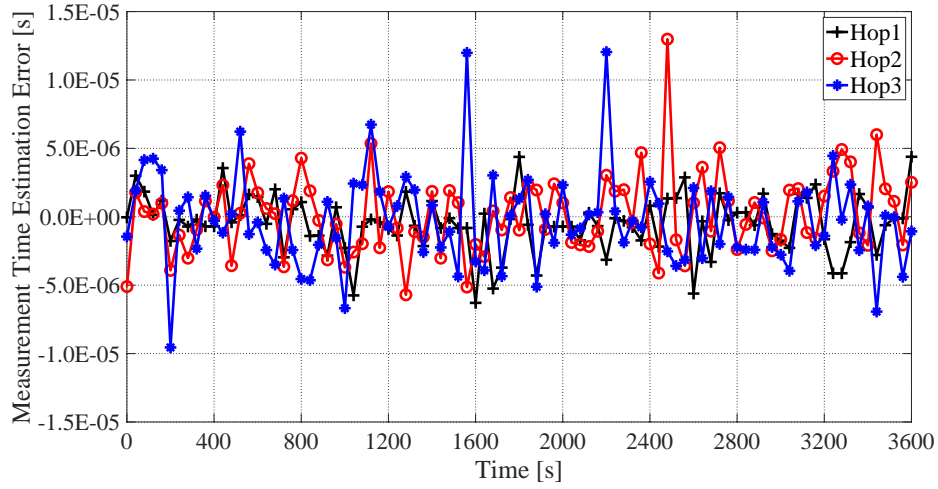
Figure 7: Measurement time estimation errors of AHTS with SI of 1 s for the multi-hop scenario.
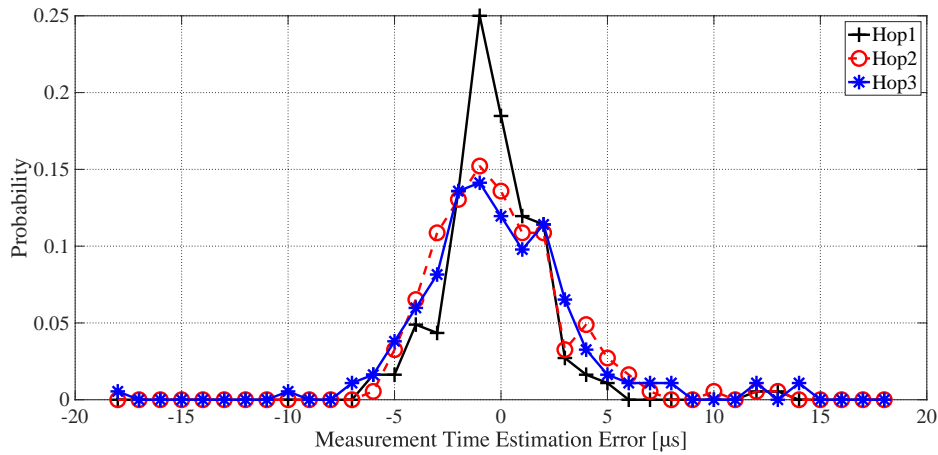

Figure 8: Probability distribution of the measurement time estimation errors of AHTS with SI of 1 s for the multi-hop scenario.

Similar behaviors are also observed in the distributions of the measurement time estimation errors shown in Fig. 8. From the figure, we can find that about 18% of the measurement time estimation errors for Hop 1 are close to zero, while this percentage of time estimation errors close to zero decreases to around 14% and 13% for Hop 2 and Hop 3, respectively. Note that most of the measurement time estimation errors are within the range of

Table 2: MAE and MSE of Measurement Time Estimation of AHTS for the Multi-Hop Scenario

Hop Number		MAE [1]	MSE [1]
Hop	3	2.5700E-06	1.2432E-11
	2	2.3648E-06	1.1056E-11
	1	2.1774E-06	9.4104E-12

[1] The samples measured between 360 s (i.e., a tenth of the observation period) and 3600 s are employed to avoid the effect of a transient period.

$-10\,\mu s$ and $10\,\mu s$ for all hop counts in Fig. 8, which demonstrates that the proposed AHTS could provide high-precision time synchronization in multi-hop networks as well as single-hop networks.

5. Conclusions

In this paper, we have investigated the actual performance of EE-ASCFR proposed in [5]—i.e., the state-of-the-art propagation delay and clock skew compensated time synchronization scheme designed to provide sub-microsecond-level synchronization accuracy—on resource-constrained sensor nodes and, based on the results of the investigation with a real WSN testbed, proposed AHTS to address the issues raised from the practical implementation of EE-ASCFR, which can achieve high-precision network-wide time synchronization even with resource-constrained sensor nodes in multi-hop topologies. Noting that the limited precision in floating-point arithmetic of the resource-constrained sensor nodes (i.e., 32-bit single-precision on a broad range of WSN platforms including motes running TinyOS and Arduino) has negative impacts on the time synchronization performance of EE-ASCFR, we move all the time synchronization tasks of sensor nodes except timestamping to the head in AHTS and apply this approach to its extension to multi-hop topologies as well.

The results of experiments for a single-hop scenario with a real WSN testbed consisting of TelosB motes running TinyOS show that the proposed AHTS consistently outperforms EE-ASCFR in terms of measurement time estimation errors by successfully addressing the issue of the precision loss in time synchronization at resource-constrained sensor nodes and can deliver microsecond-level time synchronization accuracy with all three values of SI

18

considered—i.e., 1 s, 10 s and 100 s. We have also carried out experiments for a three-hop WSN consisting of one head and three sensor nodes to investigate the effect of the number of hops on the time synchronization performance of AHTS in multi-hop topologies. The results show that the MAE of measurement time estimation for Hop 1 is 2.1774 µs, which is close to that of the single-hop scenario (i.e., 1.8166 µs), and that the MAE of measurement time estimation increases as the hop count increases by around 0.2 µs per hop. The distributions of the measurement time estimation errors from the multi-hop experiments show that most of the measurement time estimation errors are within the range of −10 µs and 10 µs for all hop counts, which demonstrates that the proposed AHTS could provide high-precision time synchronization in multi-hop networks as well as single-hop networks.

Related with our investigation in this paper on the actual performance of high-precision propagation delay and clock skew compensated time synchronization schemes on resource-constrained sensor nodes and addressing the issues raised from their practical implementation on a real WSN testbed, we have identified several areas of further investigation.

First, the scalability of AHTS needs to be studied on a testbed with a larger number of sensor nodes. Because there are lots of messages for not only timestamps but also measurements to be exchanged between the head and sensor nodes in multi-hop topologies, the bundling of measurement messages in a limited size of the payload of synchronization messages at both end and intermediate sensor nodes and their impact on the overall network traffic are to be carefully studied.

Second, as the proposed AHTS is based on EE-ASCFR designed for high energy-efficiency as well as high-precision time synchronization, the energy consumption of AHTS is to be examined with the actual measurement on a real testbed.

Note that the underlying design assumption of having a more resourceful head node in AHTS well suits to not only a variety of WSN applications but also future IoT deployments [25].

Acknowledgment

[1] P. Huang, L. Xiao, S. Soltani, M. W. Mutka, and N. Xi, "The evolution of MAC protocols in wireless sensor networks: A survey," *IEEE Commun. Surveys Tuts.*, vol. 15, no. 1, pp. 101–120, First 2013.

[2] R. C. Carrano, D. Passos, L. C. S. M. aes, and C. V. N. Albuquerque, "Survey and taxonomy of duty cycling mechanisms in wireless sensor networks," *IEEE Commun. Surveys Tuts.*, vol. 16, no. 1, pp. 181–194, First 2014.

[3] Y. Liu, D. Zhang, X. Guo, M. Gao, Z. Ming, L. Yang, and L. M. Ni, "RSS-based ranging by leveraging frequency diversity to distinguish the multiple radio paths," *IEEE Transactions on Mobile Computing*, vol. 16, no. 4, pp. 1121–1135, April 2017.

[4] D. Zhang, Y. Liu, X. Guo, and L. M. Ni, "RASS: A real-time, accurate, and scalable system for tracking transceiver-free objects," *IEEE Transactions on Parallel and Distributed Systems*, vol. 24, no. 5, pp. 996–1008, May 2013.

[5] K. S. Kim, S. Lee, and E. G. Lim, "Energy-efficient time synchronization based on asynchronous source clock frequency recovery and reverse two-way message exchanges in wireless sensor networks," *IEEE Transactions on Communications*, vol. 65, no. 1, pp. 347–359, Jan 2017.

[6] K. S. Kim, "Asynchronous source clock frequency recovery through aperiodic packet streams," *IEEE Communications Letters*, vol. 17, no. 7, pp. 1455–1458, July 2013.

[7] S. Ganeriwal, R. Kumar, and M. B. Srivastava, "Timing-sync protocol for sensor networks," in *Proc. SenSys'03*. New York, NY, USA: ACM, 2003, pp. 138–149.

[8] M. Maróti, B. Kusy, G. Simon, and Ákos Lédeczi, "The flooding time synchronization protocol," in *Proc. 2nd Int. Conf. SenSys*, New York, NY, USA, 2004, pp. 39–49.

[9] J. P. B. Nadas, R. D. Souza, M. E. Pellenz, G. Brante, and S. M. Braga, "Energy efficient beacon based synchronization for alarm driven wireless sensor networks," *IEEE Signal Processing Letters*, vol. 23, no. 3, pp. 336–340, March 2016.

[10] A. Al-Shaikhi and A. Masoud, "Efficient, single hop time synchronization protocol for randomly connected wsns," *IEEE Wireless Communications Letters*, vol. 6, no. 2, pp. 170–173, April 2017.

[11] L. Tavares Bruscato, T. Heimfarth, and E. Pignaton de Freitas, "Enhancing time synchronization support in wireless sensor networks," *Sensors*, vol. 17, no. 12, 2017. [Online]. Available: https://www.mdpi.com/1424-8220/17/12/2956

[12] F. Gong and M. L. Sichitiu, "CESP: A low-power high-accuracy time synchronization protocol," *IEEE Transactions on Vehicular Technology*, vol. 65, no. 4, pp. 2387–2396, Apr. 2016.

[13] H. Wang, L. Shao, M. Li, and P. Wang, "Estimation of frequency offset for time synchronization with immediate clock adjustment in multihop wireless sensor networks," *IEEE Internet of Things Journal*, vol. 4, no. 6, pp. 2239–2246, Dec 2017.

[14] M. Akhlaq and T. R. Sheltami, "RTSP: An accurate and energy-efficient protocol for clock synchronization in WSNs," *IEEE Transactions on Instrumentation and Measurement*, vol. 62, no. 3, pp. 578–589, March 2013.

[15] "TelosB datasheet," http://www.memsic.com/userfiles/files/Datasheets/WSN/telosb_datasheet.pdf, accessed: 08-07-2019.

[16] "Tinyos documentation wiki," http://tinyos.stanford.edu/tinyos-wiki/index.php/TinyOS_Documentation_Wiki, accessed: 08-07-2019.

[17] "MicaZ datasheet," http://www.memsic.com/userfiles/files/Datasheets/WSN/micaz_datasheet-t.pdf, accessed: 08-07-2019.

[18] "IriS datasheet," http://www.nr2.ufpr.br/~adc/documentos/iris_datasheet.pdf, accessed: 08-07-2019.

[19] "Arduino platforms," https://www.arduino.cc/, accessed: 08-07-2019.

[20] J.-P. Sheu, W.-K. Hu, and J.-C. Lin, "Ratio-based time synchronization protocol in wireless sensor networks," *Telecommunication Systems*, vol. 39, no. 1, pp. 25–35, Sep 2008.

[21] D. Djenouri and M. Bagaa, "Implementation of high precision synchronization protocols in wireless sensor networks," in *Proc. WOCC 2014*, May 2014, pp. 1–6.

[22] IEEE Computer Society, *IEEE Std 754^{TM}-2008, IEEE Standard for floating-point arithmetic*, IEEE Std., Aug. 2008.

[23] D. Gay, P. Levis, R. von Behren, M. Welsh, E. Brewer, and D. Culler, "The nesC language: A holistic approach to networked embedded systems," in *Proc. PDLI 2003*, Jun. 2003.

[24] "Float format in nesC," https://github.com/tinyos/nesc/blob/master/libiberty/floatformat.c, accessed: 08-07-2019.

[25] B. Badihi, R. Jantti, Huseyin, and Yigitler, "Time synchronization for IoT deployments: Clock discipline algorithms and protocols," https://www.researchgate.net/publication/328577639_Time_Synchronization_for_IoT_Deployments_Clock_Discipline_Algorithms_and_Protocols, Oct. 2018, accessed: 08-07-2019.